Published in final edited form as:
Circulation. 2009 January 27; 119(3): 426–435. doi:10.1161/CIRCULATIONAHA.108.785949.

Interferon-γ and the Interferon-Inducible Chemokine, CXCL10, Protect Against Aneurysm Formation and Rupture

Victoria L. King, PhD[1,2,¶], **Alexander Y. Lin, MD**[4,5,¶], **Fjoralba Kristo, MD**[4,5], **Thomas J.T. Anderson, BA**[4,5], **Neil Ahluwalia, MD**[4,5], **Gregory Hardy, BS**[4,5], **A. Phillip Owens III, BS**[1,3], **Deborah A. Howatt, BS**[1], **Dongxiao Shen, PhD**[4,5], **Andrew M. Tager, MD**[4], **Andrew D. Luster, MD, PhD**[4], **Alan Daugherty, PhD, DSc**[1,2,3], and **Robert E. Gerszten, MD**

[1]Cardiovascular Research Center, University of Kentucky, Lexington, KY

[2]Graduate Center for Nutritional Sciences, University of Kentucky, Lexington, KY

[3]Graduate Center for Toxicology, University of Kentucky, Lexington, KY

[4]Center for Immunology & Inflammatory Diseases, Massachusetts General Hospital, Charlestown, MA and Harvard Medical School, Boston, MA

[5]Cardiovascular Research Center, Massachusetts General Hospital, Charlestown, MA and Harvard Medical School, Boston, MA

Abstract

Background—Vascular disease can manifest as stenotic plaques or ectatic aneurysms, though the mechanisms culminating in these divergent disease manifestations remain poorly understood. T helper type 1 (Th1) cytokines, including interferon (IFN)-γ and CXCL10, have been strongly implicated in atherosclerotic plaque development.

Methods and Results—Here we specifically examined their role in the formation of abdominal aortic aneurysms (AAA) in the angiotensin (Ang)II-induced murine model. Unexpectedly, we found increased suprarenal aortic diameters, AAA incidence and aneurysmal death in *Apoe*$^{-/-}$/*Ifng*$^{-/-}$ mice compared to *Apoe*$^{-/-}$ controls, though atherosclerotic luminal plaque formation was attenuated. The IFN-γ-inducible T cell chemoattractant CXCL10 was highly induced by AngII infusion in *Apoe*$^{-/-}$ mice, but this induction was markedly attenuated in *Apoe*$^{-/-}$/*Ifng*$^{-/-}$ mice. *Apoe*$^{-/-}$/*Cxcl10*$^{-/-}$ mice had decreased luminal plaque, but also increased aortic size, worse morphological grades of aneurysms, and a higher incidence of death due to aortic rupture than *Apoe*$^{-/-}$ controls. Furthermore, AAAs in *Apoe*$^{-/-}$/*Cxcl10*$^{-/-}$ mice were enriched for non-Th1 related signals, including transforming growth factor (TGF)-β1. Treatment of *Apoe*$^{-/-}$/*Cxcl10*$^{-/-}$ mice with anti-TGF-β neutralizing antibody diminished AngII-induced aortic dilation.

*Correspondence should be addressed to: Robert E. Gerszten, M.D., Cardiology Division and Center for Immunology & Inflammatory Diseases, Massachusetts General Hospital – East Campus, 149 13th Street, Room 8307, Charlestown, MA 02129, Office: 617-724-8322, Fax: 617-726-5651, rgerszten@partners.org.
¶Denotes Equal Contribution

A wealth of recent findings suggest that inflammation contributes to vascular disease. However, our understanding of the precise mechanisms involved remains incomplete. The present study defines a novel pathway in which two related inflammatory mediators, IFN-γ and CXCL10, contribute to plaque formation in arteries--but protect against the formation of vessel aneurysms. Thus, efforts to develop anti-inflammatory strategies for atherosclerosis must carefully consider potential effects on all types of vascular disease manifestations, and consider both the salutary and harmful aspects of the immune system.

Conflict of Interest Disclosures
None.

Conclusion—The present study defines a novel pathway in which IFN-γ and its effector, CXCL10, contribute to divergent pathways in AAA versus plaque formation, inhibiting the former pathology but promoting the latter. Thus, efforts to develop anti-inflammatory strategies for atherosclerosis must carefully consider potential effects on all manifestations of vascular disease.

Keywords

aneurysm; atherosclerosis; immunology; inflammation; knockout mice

Introduction

The pathophysiological mechanisms that lead to stenotic plaques versus aneurysms, two distinct vascular lesions, remain poorly understood. Clinically, abdominal aortic aneurysms (AAA) are more strongly correlated with a family history[1] and smoking[2] than are coronary stenoses. Diabetes, a strong risk factor for coronary plaques, actually protects against AAA formation in population-based studies.[3,4]

Chronic inflammation of the vascular wall is believed to contribute to both manifestations of arterial pathology.[5,6] Atherosclerotic plaques are marked primarily by intimal infiltration of macrophages and T cells, at least at earlier disease stages. In contrast, aneurysmal segments are characterized by macrophage, T cell, and B cell accumulation primarily in the media and adventitia at all stages of disease evolution.[6] Human atherosclerotic stenoses specifically express mediators characteristic of a T helper type 1 (Th1) immune response, including interferon (IFN)-γ, as well as the IFN-γ-inducible T cell chemoattractant, IP-10 (IFN-γ-inducible Protein of 10 kiloDaltons, now known as CXCL10).[7] Characterization of mediators expressed by AAAs, however, has been inconsistent, which is potentially attributable to different disease stages and anatomical areas studied. Tang et al. found transmural accumulation of IFN-γ producing T cells correlating with aortic dilation,[8] though other groups have described a Th2 predominant immune response prevailing in human AAA.[6,9]

$CD4^+$ T cell deletion protects against AAA formation in a calcium chloride-induced AAA model in mice.[10] However, murine studies to date have not clarified whether adaptive cellular immunity of either the Th1 or Th2 system is detrimental or beneficial in aneurysmal disease. While the Th1 cytokine interferon-γ contributes to atherosclerotic plaque formation,[11] there are conflicting reports on the role of IFN-γ and its receptor on the development of AAAs. IFN-γ deficiency resulted in a modest reduction of disease pathology in the calcium chloride-induced AAA model, while IFN-γ infusion restored the severity of the disease.[10] In contrast, IFN-γ receptor deficiency augmented AAA formation in an aortic allograft model of AAA formation.[12] These seemingly contradictory studies may be less surprising in light of an emerging theme of proinflammatory and regulatory interplay of IFN-γ in inflammation and autoimmunity in other disease models, including arthritis[13] and multiple sclerosis.[14,15] IFN-γ appears to act as a master upstream regulator modulating both pro- and anti-inflammatory processes depending on the disease stage and disease-specific cytokines.

Complete ablation of IFN-γ signaling, like global T cell deletion, might thus disturb both effector and regulatory arms of the immune system, potentially resulting in variable effects on vascular phenotypes. In contrast, a disruption that isolates specific downstream pathways might be particularly informative regarding the signals contributing to AAA. We therefore studied AAA formation both in IFN-γ-deficient mice and in mice deficient in the IFN-γ-inducible T cell chemokine, CXCL10. These studies define a novel role for CXCL10 in AAA formation and more broadly suggest that cellular immunity may play different roles in two distinct manifestations of vascular disease, with important clinical implications.

Methods

Mice

Apoe$^{-/-}$, *Ifng*$^{-/-}$ mice (Jackson Laboratory, Bar Harbor, ME), and *Cxcl10*$^{-/-}$ mice[16] were backcrossed 10 times into a C57BL/6J background, and inter-bred to generate the experimental genotypes, which were confirmed by PCR genotyping. All mice received a standard laboratory diet (Harlan Teklad). All animal procedures were approved by university animal care protocols at their respective institutions (University of Kentucky; Massachusetts General Hospital).

Infusion of angiotensin II (AngII)

Experimental mice were treated with AngII (500 or 1000 ng·kg^{-1}·min^{-1} as indicated, Sigma Chemical Co.) or normal saline via ALZET Model 2004 osmotic pumps (DURECT Corporation) that were implanted subcutaneously as described previously.[17] After 4 weeks of infusion, mice were sacrificed for blood collection and aorta harvest.

Lipid analysis

A total of 0.5 to 1.0 mL of blood was aspirated from experimental mice by right ventricular puncture upon euthanasia. Serum cholesterol concentrations were measured by enzymatic colorimetric assay (Wako Chemical Company). Lipoprotein-cholesterol distribution was determined in individual serum samples (50 μl) from mice following resolution on a Superose 6 column.[18]

Blood pressure measurements

Systolic blood pressure was measured serially in conscious mice using a tail-cuff system (Visitech BP-2000 or Kent Scientific XBP1000) during three training sessions at baseline and four weeks following the placement of the AngII pump.

Atherosclerotic lesion analysis

The size of atherosclerotic lesions was quantified using Image-Pro software (Media Cybernetics).[19] Discernable lesions on the luminal surface of the aorta were quantified from the aortic arch to the last intercostal artery branch in the thorax.

Quantification of aneurysms and morphometric analysis

Aortic diameters and AAA incidence were determined as described previously.[17] The maximum width of abdominal aortas was measured using computerized morphometry. Aneurysm incidence was quantified based on a definition of an external suprarenal aorta width that was increased by 50% or greater compared to saline-infused mice. In addition, we used a previously described classification[20,21] to categorize the morphological grade of the aneurysms: no aneurysm, Type I (suprarenal dilation without thrombus), Type II (remodeled suprarenal dilation with thrombus), Type III (multiple aneurysms, including thoracic aneurysms and dissections), and death due to aneurysmal rupture. On necropsies of unexpected deaths, death due to rupture of an aneurysm was qualified by presence of a retroperitoneal hematoma in addition to an abdominal aortic aneurysm, and/or presence of a thoracic hematoma in addition to a thoracic aortic aneurysm or dissection. Measurements were conducted by two trained, independent observers blinded to genotype and treatment conditions.

Antibodies and immunohistochemistry (IHC) of murine lesions

For harvesting suprarenal aortas for IHC, mice were perfused via left ventricular puncture with 4% paraformaldehyde (PFA) under physiologic pressure and aortic segments were embedded in Optimal Cutting Tissue (OCT) compound (Tissue-Tek). Serial 10 μm sections were cut

surrounding the cross-section of widest diameter and every fifth section was stained. Tissues were stained with hematoxylin and eosin (H & E, Fisher Scientific) for morphology. IHC was performed with antibodies to identify macrophages (Mac3, 1:20, BD Biosciences), $CD4^+$ T cells (CD4, 1:50, BD Pharmingen), Thy-1.2^+ T cells (CD90.2; BD Pharmingen), VSMCs (α-actin, 1:100, Abcam), as well as CXCL10 (1:100, R&D Systems). Negative controls were prepared with substitution of the primary antibody with an isotype-matched control antibody. Appropriate biotinylated secondary antibodies were used, followed by detection with ABC Development Kit (Vector Laboratories) and color development with DAB (Chemicon) or AEC (Dako). High-powered fields (HPFs) of stained sections were randomly captured using a SPOT digitizer (Diagnostic Instruments) and quantitative analysis was performed with IP Lab (BD Biosciences) by a single observer blinded to genotype and condition. Areas positively stained were divided by total lesion area to account for variability in lesion size.

To assess TGF-β activity, we used a polyclonal antibody specific for the free and active form of TGF-β.[22,23] To test the role of TGF-β in AAA formation in *Apoe*$^{-/-}$ and *Apoe*$^{-/-}$/*Cxcl10*$^{-/-}$ mice, mice were injected intraperitoneally one day prior to the placement of the AngII pump and one day after pump placement with a pan-specific neutralizing antibody against TGF-β1, 2, and 3, (1 mg/kg, R&D Systems, Minneapolis)[24] or isotype control.

RNA isolation and quantitative PCR

Total RNA was isolated from suprarenal aortas from mice perfused with RLT Buffer (Applied Biosystems) using mechanical homogenization with a roto-stator and RNeasy columns (Qiagen).[25,26] After DNaseI digestion, equivalent amounts of RNA from each sample were reverse transcribed using Taqman reverse-transcription reagents, including oligo $(dT)_{15}$, random hexamers, and Multiscribe reverse transcriptase (Applied Biosystems). Quantitative (q) RT-PCR reactions were conducted with the Multiplex qPCR system as described.[25,26] Amplification plots were analyzed with MX4000 software, version 3.0. Gene expression was normalized to GAPDH or β-actin as an internal control.

Vascular contractility experiments—Abdominal aortas were removed and cleaned of adventitia while immersed in Kreb's buffer. Measurement of force contraction was performed at 37°C as described previously.[27] Briefly, abdominal aortic segments (3 mm) were mounted by passing two tungsten wires through the arterial lumen and bathed in wells (Kent Scientific) filled with Krebs Henseleit solution. Tension (1 gm) was maintained continuously and recorded using a Tissue Force Analyzer 410 (Micro-Med Instruments). After 30 min equilibration, abdominal aortic segments were immersed in potassium chloride (80 mM) for 3 min. After washout and 30 minutes equilibration, contractile activity was determined during incubation with phenylephrine (PE; Sigma; 1 nM - 1 mM).

Statistical analysis

Data were analyzed by two-way ANOVA, Student's *t* test, Chi-square, or Mann-Whitney Rank Sum using SigmaStat. Data were tested for use of parametric or non-parametric post hoc analysis and multiple comparisons were performed using Tukey or Holm-Sidak tests, as appropriate for the data. Percent incidence of AAAs was analyzed by Fisher's exact test. $P < 0.05$ values were considered to be statistically significant. All data are represented as means ± standard error of means (SEM).

Statement of Responsibility

The authors had full access to and take full responsibility for the integrity of the data. All authors have read and agree to the manuscript as written.

Results

Increased IFN-γ and CXCL10 mRNA expression in AngII-infused Apoe$^{-/-}$ mice

Mice were placed on a normal diet for 20 weeks and then treated with AngII (1000 ng·kg^{-1}·min^{-1}) or vehicle control via Alzet osmotic pumps for 4 weeks, which generates AAA in a reproducible manner and mimics many of the important features of the human disease.[17,28] AngII infusion did not generate any AAA in control C57BL/6J mice (data not shown). Quantitative real-time polymerase chain reaction (qPCR) analysis of suprarenal aortic segments revealed significantly higher expression of the Th1-associated cytokines IFN-γ and CXCL10 (as well as its receptor CXCR3), in the AngII-exposed *Apoe*$^{-/-}$ mice as compared to the saline-treated controls (Figure 1). C57BL/6J mice had similar trends for CXCL10 and CXCR3, but overall expression levels were markedly lower.

IFN-γ deficiency has contrasting effects on AngII-induced AAA and atherosclerosis formation

To address the role of IFN-γ in AAA formation, we infused 20-week old *Apoe*$^{-/-}$ mice that were either *Ifng*$^{+/+}$ or *Ifng*$^{-/-}$ with AngII (1000 ng·kg^{-1}·min^{-1}) or saline. Unexpectedly, 50% of the *Apoe*$^{-/-}$/*Ifng*$^{-/-}$ mice died due to rupture of the abdominal aorta within 2 to 10 days of AngII infusion (Figure 2 and Supplemental Figure 1). In contrast, there were no deaths due to aneurysmal rupture in the *Apoe*$^{-/-}$/*Ifng*$^{+/+}$ group. Due to the high incidence of mortality in *Apoe*$^{-/-}$/*Ifng*$^{-/-}$ mice, the infusion of AngII was decreased to 500 ng·kg^{-1}·min^{-1} for subsequent studies of this genotype.

Total serum cholesterol concentrations were not altered by IFN-γ deficiency in either saline or AngII-infused mice (Table 1). IFN-γ deficiency did not alter systolic blood pressure prior to or during infusion of AngII (data not shown). IFN-γ deficiency led to increased body weight in the *Apoe*$^{-/-}$ background, though body weight was unaffected by AngII infusion (Table 1). Adiponectin levels were not different between *Apoe*$^{-/-}$/*Ifng*$^{-/-}$ mice and *Apoe*$^{-/-}$ mice (n=9 of each; P=0.67), thus excluding one potentially confounding modifier of vascular pathology.[29]

With the lower dose infusion of AngII (500 ng·kg^{-1}·min^{-1}), we observed significantly increased suprarenal aortic diameters in *Apoe*$^{-/-}$/*Ifng*$^{-/-}$ mice as compared to *Apoe*$^{-/-}$ controls (Figure 3A; P<0.05). IFN-γ-deficient mice also had a concordant increase in the incidence of AAAs as compared to the *Ifng*$^{+/+}$ controls (*Apoe*$^{-/-}$ /*Ifng* $^{-/-}$, 18 of 29 mice, 62% incidence; versus *Apoe*$^{-/-}$, 8 of 25 mice, 32% incidence; P<0.05, Figure 3B). No AAAs were present in saline-infused control mice. Of note, IFN-γ deficiency did not produce any discernable differences in medial area or thickness of the suprarenal aorta (Supplemental Figures 2A and 2B), ruling out preexisting vascular differences between these genotypes that might predispose *Apoe*$^{-/-}$ /*Ifng* $^{-/-}$ mice to AAA. Furthermore, in functional assays IFN-γ deficiency did not impart any significant differences in the ability of the abdominal aorta to respond to KCl or phenylephrine (Supplemental Table 1). Thus, despite IFN-γ deficiency leading to dramatic differences in aneurysm formation in the suprarenal aorta, this was not associated with discernable structural or functional changes in the vessel wall.

Luminal atherosclerotic lesions were also quantified in mice infused with AngII or saline. Minimal lesion development was noted in saline-infused mice fed a normal diet (Figure 4, left panel). Consistent with previous reports, AngII infusion markedly enhanced atherosclerotic lesion size (Figure 4, right panel).[17,30] However, as in hyperlipidemic-induced atherosclerosis, AngII-induced lesion formation was attenuated by IFN-γ deficiency (P<0.05). Thus, IFN-γ deficiency had a differential effect on atherosclerotic lesion formation as opposed to AAA formation.

CXCL10 deficiency has contrasting effects on AngII-induced AAA and atherosclerosis formation

CXCL10 is an IFN-γ-inducible, effector T cell chemokine that was highly upregulated by AngII infusion in *Apoe*$^{-/-}$ mice (Figure 1). CXCL10 expression appeared to be highest in the media and adventitia, suggesting that its role in the recruitment of T cells was likely occurring from the adventitia and neovessels, and not from the aortic lumen. Consistent with our prior studies,[31] we observed down-regulation of CXCL10 in spleens and vascular lesions of hyperlipidemic, IFN-γ-deficient mice (Figures 5A and 5B). Like *Apoe*$^{-/-}$/*Ifng*$^{-/-}$ mice,[32] CXCL10-deficient mice in the ApoE background on a high fat diet were also recently found to have a greater than two-fold reduction in atherosclerotic plaques compared to controls.[33] We thus explored the role of CXCL10 in atherosclerotic plaque development and AAA formation in the AngII model. 20-week old *Apoe*$^{-/-}$ and *Apoe*$^{-/-}$/*Cxcl10*$^{-/-}$ mice received AngII (1000 ng·kg^{-1}·min^{-1}) or saline for 28 days. At sacrifice, *Apoe*$^{-/-}$ and *Apoe*$^{-/-}$/*Cxcl10*$^{-/-}$ mice had similar lipid profiles (Table 2). The AngII-infused *Apoe*$^{-/-}$/*Cxcl10*$^{-/-}$ mice weighed slightly more than their age-matched *Apoe*$^{-/-}$ controls (Table 2), but had no differences in adiponectin levels (n=7 of each, P=0.21).

CXCL10 deletion protected against atherosclerotic luminal plaque formation in the AngII model (Figure 5C), consistent with prior results on a high fat diet.[33] While luminal plaque formation was diminished, *Apoe*$^{-/-}$/*Cxcl10*$^{-/-}$ mice had a significantly higher death rate due to aortic rupture than the *Apoe*$^{-/-}$ controls in the AngII-triggered AAA model (42% vs. 11%; P<0.01, Figure 6A; representative necropsy in Supplemental Figure 3). We were interested to find that the rate of rupture in the *Apoe*$^{-/-}$/*Cxcl10*$^{-/-}$ mice was comparable to that observed in the *Apoe*$^{-/-}$/*Ifng*$^{-/-}$ mice. Concordant with the increased mortality observed in the *Apoe*$^{-/-}$/*Cxcl10*$^{-/-}$ double knockouts, we also documented more severe morphological changes throughout the aortas of these mice than *Apoe*$^{-/-}$ controls (Figure 6B). Whereas *Apoe*$^{-/-}$ controls had localized suprarenal AAAs, the *Apoe*$^{-/-}$/*Cxcl10*$^{-/-}$ mice had thoracic aneurysms and hematomas with and without abdominal aneurysms, as well as large aneurysms with spiral dissections. Consistently, the infrarenal aorta had no aneurysmal pathology in either genotype (though occasionally the aortic segment between the renal arteries was involved in conjunction with a suprarenal AAA), agreeing with previous reports.[34] We quantified these morphological differences using a previously reported classification grade that accounts for the complexity and multiplicity of the aneurysms.[20,21] The distribution of grades was different between the two genotypes (Figure 6C, P< 0.005), with the *Apoe*$^{-/-}$/*Cxcl10*$^{-/-}$ having significantly more Grade III aneurysms or death due to rupture of the aorta. Similar to the findings in the IFN-γ-deficient mice, we also observed significantly increased suprarenal diameters and suprarenal/thoracic-to-infrarenal aortic area ratios in the *Apoe*$^{-/-}$/*Cxcl10*$^{-/-}$ mice as compared to the *Apoe*$^{-/-}$ controls (Figures 6D and 6E). Of note, these analyses may underestimate differences between the two genotypes since mortality was substantially increased in the *Apoe*$^{-/-}$/*Cxcl10*$^{-/-}$ mice and therefore some aneurysms were not incorporated into the analyses represented by Figures 6D and 6E.

Taken together, the *Apoe*$^{-/-}$/*Cxcl10*$^{-/-}$ mice had qualitatively and quantitatively worse aneurysmal disease with elements of remodeling, dilation, and rupture, involving more of the aorta than previously reported with this model. Thus, deficiency of either IFN-γ or the IFN-γ-inducible chemokine, CXCL10, yielded exacerbation of AAA pathology, despite there being diminished plaque formation in the absence of either of these cytokines.

Reduction of T cell accumulation in CXCL10-deficient aneurysms

We next performed immunohistochemical studies of aortic vessel wall constituents to further delineate the effects of CXCL10 deletion on AAA formation. As previously reported, cross-sectional histology demonstrated lumen dilation, breaks in medial elastin, as well as thrombus

formation.[28] Consistent with deletion of the effector T lymphocyte chemokine, CXCL10, we documented a significant decrease in $CD4^+$ T lymphocyte accumulation in the suprarenal AAA of the *Apoe*$^{-/-}$/*Cxcl10*$^{-/-}$ mice as compared to *Apoe*$^{-/-}$ controls, as assessed both by quantitative PCR and by immunohistochemical analysis (Figures 7A–7C). There was a concordant reduction in mRNA for the CXCL10 receptor, CXCR3, consistent with decreased infiltration of effector T cells (P=0.004, Figure 7D).[7,35] Also consistent with the decreased accumulation of activated T lymphocytes in particular, we observed a concomitant reduction in IFN-γ production within the vessel wall as assessed by qPCR (Figure 7E). Interestingly, there was also a significant decrease in macrophage accumulation in the arterial wall of the *Apoe*$^{-/-}$/*Cxcl10*$^{-/-}$ double knockout mice as compared to *Apoe*$^{-/-}$ controls (data not shown). Since CD4 is present at very low levels on macrophages, we also performed immunostaining with an anti-Thy-1.2 antibody, which confirmed the reduction in T cells in the lesions (Supplemental Figure 4).

TGF-β1 blockade inhibits AAA size in CXCL10-deficient mice

We hypothesized that in the absence of IFN-γ and CXCL10, the lesional cytokine milieu would be enriched for non-Th1 related signals, such as TGF-β1. Recent studies have also demonstrated that TGF-β1 activation appears to potentiate aortic root aneurysm formation in murine models of Marfan syndrome.[24] In this context, we found that *Apoe*$^{-/-}$/*Cxcl10*$^{-/-}$ aneurysmal sections contained significantly greater amounts of activated TGF-β, as assessed by immunohistochemical analysis with an activation-specific TGF-β antibody[36] (Figures 8A and 8B). Furthermore, inhibition of TGF-β activity with a neutralizing antibody[24] significantly diminished aortic area in the CXCL10-deficient mice treated with AngII for two weeks (Figure 8C).

Discussion

Here we specifically explored the roles of IFN-γ and CXCL10 in the formation of AAA. While AngII-induced atherosclerotic lesion formation was attenuated in IFN-γ-deficient mice, there was an unexpected increase in suprarenal aortic diameter and AAA incidence. The IFN-γ-inducible effector T cell chemokine, CXCL10, which is highly up-regulated by AngII infusion in *Apoe*$^{-/-}$ mice--and down-regulated in the setting of IFN-γ-deficiency--also conferred protection from AAA formation. Compared to the *Apoe*$^{-/-}$ control mice, compound deficient *Apoe*$^{-/-}$/*Cxcl10*$^{-/-}$ mice had increased aortic size, worse morphological grades of aneurysms, and a higher incidence of death due to aortic rupture. The aortas of *Apoe*$^{-/-}$/*Cxcl10*$^{-/-}$ mice were characterized by downregulation of IFN-γ, and upregulation of the pro-aneurysmal growth factor TGF-β1. Furthermore, inhibition of TGF-β with a neutralizing antibody diminished aortic area in the AngII-triggered model.

While clinical evidence suggests that coronary atherosclerosis and AAA formation share some common features, important differences exist, such as the discordant effect of diabetes on the prevalence of these two disease manifestations. A prominent inflammatory component is common to both vascular pathologies, though histological analyses also show differences. Coronary atherosclerosis is marked specifically by the accumulation of a Th1 type immune response.[7] In contrast, studies of AAA have found evidence for both Th1 and Th2 type responses.[8,12] Prior studies have hinted at molecular signals differing in aneurysmal versus stenotic vascular disease. For example, genetic deficiency of matrix metalloproteinase (MMP)-3, tissue inhibitor of metalloproteinases-1, or 5-lipoxygenase, and pharmacological inhibition of MMPs in hyperlipidemic mice have had variable effects on atherosclerosis as compared to AAA formation.[37–40] The present study extends prior work by defining a novel pathway in which IFN-γ and its effector, CXCL10, lead to discordant effects in the two vascular disease processes. Thus, while multiple lines of investigation have shown that T helper type 1

(Th1) cells and their related pro-inflammatory cytokines promote atherogenesis, we show that these same cytokines protect against the formation of abdominal aortic aneurysms (AAA) in a well-characterized murine system.

An extensive literature documents the function of IFN-γ in potentiating the inflammatory response. However, more recent evidence suggests that IFN-γ also plays a role in the resolution of inflammatory processes. Data supporting the complex role of IFN-γ have come both from antibody blocking experiments and from attempts to induce autoimmune inflammation in IFN-γ and IFN-γ receptor knockout mice. For example, increased disease severity was documented in mouse models of multiple sclerosis and collagen-induced arthritis using animals deficient for IFN-γ or the IFN-γ receptor.[13–15] Our data are therefore consistent with the emerging notion of IFN-γ as a master regulator, upstream of multiple pathways that evolve during the disease process. With regards specifically to vascular biology, the contrasting effects of IFN-γ deficiency on AAA and stenotic vascular disease may be attributed to localization of these diseases to different layers of the aorta. Additionally, differences in the temporal accumulation of different cell types and presence of different cytokines and growth factors might account for the opposing effect of IFN-γ deficiency on atherosclerosis and aneurysms.

We observed significantly increased levels of TGF-β1 in the AngII-induced AAA of *Apoe*$^{-/-}$*/Cxcl10*$^{-/-}$ double knockout mice as compared to the *Apoe*$^{-/-}$ controls. This finding is consistent with our prior studies in which we found enhanced expression of non-Th1 cytokines, including TGF-β1, in the diet-induced atherosclerotic plaques of CXCL10-deficient mice, despite overall diminished T cell accumulation.[33] We were particularly interested to find increases in TGF-β1 activation in AngII-infused *Apoe*$^{-/-}$*/Cxcl10*$^{-/-}$ double knockout mice in light of recent studies demonstrating the role of TGF-β1 in aortic root aneurysm formation in murine models of Marfan syndrome.[24] Investigators now postulate that fibrillin-1 tonically inhibits TGF-β1 signaling in the vessel wall. In Marfan syndrome, mutations in fibrillin-1 lead to enhanced TGF-β1 activation and ultimately vascular dilation. Furthermore, aneurysm formation in mice expressing a fibrillin mutation characteristic of human Marfan syndrome is inhibited by a TGF-β blocking antibody or by the angiotensin II type 1 receptor blocker, Losartan,[24] though there are likely to be important differences in pathways triggered in the hyperlipemia and AngII-induced aneurysm model as opposed to the genetically induced Marfan model. Our working model is that CXCL10, an IFN-γ-dependent chemokine, modulates the recruitment of effector T cells. The recruitment of T cells influences the local T cell cytokine profile in the vessel wall—including the expression of additional IFN-γ. We have demonstrated that when CXCL10 is deleted the recruitment of effector T cells is diminished, and the local cytokine milieu shifts away from a Th1 profile, leading to an enrichment of signals including TGF-β1. Growth factors such as TGF-β1 activate fibroblasts and other cell types and elicit further TGF-β1 and cytokine generation,[41] which may serve to amplify the initial changes in the cytokine profile. In atherosclerosis, shifting the balance away from Th1 cytokines with upregulation of TGF-β1 inhibits luminal plaque formation. However, TGF-β1 induction has been demonstrated to be a critical mechanism in aneurysmal dilation. Characterization of the downstream targets of TGF-β1 responsible for these discordant effects in the vasculature merits future investigation. Of note, there is precedent for TGF-β1 activity having dramatically different effects on specific aspects of disease pathology, such as mitigating inflammation but contributing to dysregulated tissue repair.[42]

Several findings of the present study potentially contrast with previous work. Whereas studies defining the effects of IFN-γ on atherosclerosis have been uniform, there are conflicting reports on the role of IFN-γ in aneurysmal-associated disease models. Blockade of IFN-γ signaling using IFN-γ receptor-deficient mice increased AAA formation in an aortic allograft model of the disease,[12] which is in agreement with the present study. However, investigators have demonstrated that increases in the abdominal aortic diameter of C57BL/6J mice triggered by

intraperitoneal administration of calcium chloride were attenuated by IFN-γ deficiency.[10] One other study has found that adenovirally-mediated overexpression of TGF-β1 attenuated aortic dilation of sodium dodecyl sulfate-treated guinea pig xenografts transplanted into Lewis rats.[43] Finally, a recent report suggests that CXCR3 (the receptor for CXCL10) deficiency has no significant effect on calcium chloride-triggered aortic dilation.[44] We would postulate that the marked differences between our model and prior systems account for the contrasting findings. The present studies utilized an AngII-treated hyperlipidemic murine model on the C57BL/6J background, which differs significantly from the prior studies which used either surgical intervention to apply calcium chloride to the external surface of the vessel or aortic transplantation to trigger AAA formation. Finally, we note that while our data highlight a role for IFN-γ and effector T cells in AAA formation, recent findings have also suggested a role for other types of IFN-γ-producing cells such as mast cells in AAA generation.[45]

Limitations to the present study must also be considered. There is considerable debate regarding the fidelity of the most commonly used AAA mouse models (adventitial calcium chloride, intra-lumen porcine elastase, subcutaneous AngII-infusion) for the human disease. The task of assessing the relevance of any of these commonly used mouse models is made difficult by our lack of knowledge of the initiation and formative stages of human AAAs. Unfortunately, the most accessible human AAA tissue is from advanced lesions that have been resected during open surgical repair, providing limited insight into the earlier stages. Despite these formidable barriers to validating any of the murine models, there are some indications that the renin-angiotensin system in particular is involved in the formation of human AAAs. Components of the renin-angiotensin system are highly expressed in human AAA tissue, particularly angiotensin converting enzyme (ACE) and chymase 3.[46] Retrospective clinical analyses have revealed that ACE inhibition is associated with reduced AAA rupture.[47] Finally, there are emerging genetic association studies linking specific AT1 receptor and ACE polymorphisms with AAA as well.[48,49]

Experimental studies are only beginning to clarify the functional role of adaptive immunity in stenotic vascular occlusive disease and AAA formation. The prevailing dogma is that Th1 immune responses contribute in a causal manner to atherosclerosis in general, but particularly with regards to luminal atherosclerotic plaque buildup. In striking contrast, our findings clearly demonstrate that two major Th1-associated cytokines, IFN-γ and CXCL10, play a protective role in AAA formation. Our data suggest that local modulation of CXCL10 represents a potential therapeutic strategy for AAA. Most importantly, the present study also suggests that efforts to develop anti-inflammatory strategies for atherosclerosis must carefully consider potential effects on all types of vascular disease manifestations, and consider both salutary and harmful aspects of the immune system.

Supplementary Material

Refer to Web version on PubMed Central for supplementary material.

Acknowledgements

Funding Sources:

The authors gratefully acknowledge support from the NIH to AD (HL62846 and HL 80100), ADL (CA069212), and REG (HL65584), and the American Heart Association (Grant-in-Aid) to REG. REG is also supported by the Donald W. Reynolds Foundation and the Leducq Foundation.

References

1. Frydman G, Walker PJ, Summers K, West M, Xu D, Lightfoot T, Codd C, Dique T, Nataatmadja M. The value of screening in siblings of patients with abdominal aortic aneurysm. Eur J Vasc Endovasc Surg 2003;26:396–400. [PubMed: 14512002]
2. Lederle FA, Nelson DB, Joseph AM. Smokers' relative risk for aortic aneurysm compared with other smoking-related diseases: a systematic review. J Vasc Surg 2003;38:329–334. [PubMed: 12891116]
3. Lederle FA, Johnson GR, Wilson SE, Chute EP, Hye RJ, Makaroun MS, Barone GW, Bandyk D, Moneta GL, Makhoul RG. The aneurysm detection and management study screening program: validation cohort and final results. Aneurysm Detection and Management Veterans Affairs Cooperative Study Investigators. Arch Intern Med 2000;160:1425–1430. [PubMed: 10826454]
4. Blanchard JF, Armenian HK, Friesen PP. Risk factors for abdominal aortic aneurysm: results of a case-control study. Am J Epidemiol 2000;151:575–583. [PubMed: 10733039]
5. Thompson RW, Geraghty PJ, Lee JK. Abdominal aortic aneurysms: basic mechanisms and clinical implications. Curr Probl Surg 2002;39:110–230. [PubMed: 11884965]
6. Shimizu K, Mitchell RN, Libby P. Inflammation and cellular immune responses in abdominal aortic aneurysms. Arterioscler Thromb Vasc Biol 2006;26:987–994. [PubMed: 16497993]
7. Mach F, Sauty A, Iarossi AS, Sukhova GK, Neote K, Libby P, Luster AD. Differential expression of three T lymphocyte-activating CXC chemokines by human atheroma-associated cells. J Clin Invest 1999;104:1041–1050. [PubMed: 10525042]
8. Tang PC, Yakimov AO, Teesdale MA, Coady MA, Dardik A, Elefteriades JA, Tellides G. Transmural inflammation by interferon-gamma-producing T cells correlates with outward vascular remodeling and intimal expansion of ascending thoracic aortic aneurysms. Faseb J 2005;19:1528–1530. [PubMed: 16014397]
9. Schonbeck U, Sukhova GK, Gerdes N, Libby P. T(H)2 predominant immune responses prevail in human abdominal aortic aneurysm. Am J Path 2002;161:499–506. [PubMed: 12163375]
10. Xiong W, Zhao Y, Prall A, Greiner TC, Baxter BT. Key roles of CD4+ T cells and IFN-gamma in the development of abdominal aortic aneurysms in a murine model. J Immunol 2004;172:2607–2612. [PubMed: 14764734]
11. Hansson GK, Libby P. The immune response in atherosclerosis: a double-edged sword. Nat Rev Immunol 2006;6:508–519. [PubMed: 16778830]
12. Shimizu K, Shichiri M, Libby P, Lee RT, Mitchell RN. Th2-predominant inflammation and blockade of IFN-gamma signaling induce aneurysms in allografted aortas. J Clin Invest 2004;114:300–308. [PubMed: 15254597]
13. Ferber IA, Brocke S, Taylor-Edwards C, Ridgway W, Dinisco C, Steinman L, Dalton D, Fathman CG. Mice with a disrupted IFN-gamma gene are susceptible to the induction of experimental autoimmune encephalomyelitis (EAE). J Immunol 1996;156:5–7. [PubMed: 8598493]
14. Vermeire K, Heremans H, Vandeputte M, Huang S, Billiau A, Matthys P. Accelerated collagen-induced arthritis in IFN-gamma receptor-deficient mice. J Immunol 1997;158:5507–5513. [PubMed: 9164974]
15. Manoury-Schwartz B, Chiocchia G, Bessis N, Abehsira-Amar O, Batteux F, Muller S, Huang S, Boissier MC, Fournier C. High susceptibility to collagen-induced arthritis in mice lacking IFN-gamma receptors. J Immunol 1997;158:5501–5506. [PubMed: 9164973]
16. Tager AM, Dufour JH, Goodarzi K, Bercury SD, von Andrian UH, Luster AD. BLTR mediates leukotriene B(4)-induced chemotaxis and adhesion and plays a dominant role in eosinophil accumulation in a murine model of peritonitis. J Exp Med 2000;192:439–446. [PubMed: 10934232]
17. Daugherty A, Manning MW, Cassis LA. Angiotensin II promotes atherosclerotic lesions and aneurysms in apolipoprotein E-deficient mice. J Clin Invest 2000;105:1605–1612. [PubMed: 10841519]
18. Heller EA, Liu E, Tager AM, Sinha S, Roberts JD, Koehn SL, Libby P, Aikawa ER, Chen JQ, Huang P, Freeman MW, Moore KJ, Luster AD, Gerszten RE. Inhibition of atherogenesis in BLT1-deficient mice reveals a role for LTB4 and BLT1 in smooth muscle cell recruitment. Circulation 2005;112:578–586. [PubMed: 16043658]

19. King VL, Szilvassy SJ, Daugherty A. Interleukin-4 deficiency decreases atherosclerotic lesion formation in a site-specific manner in female LDL receptor−/− mice. Arterioscler Thromb Vasc Biol 2002;22:456–461. [PubMed: 11884290]
20. Daugherty A, Manning MW, Cassis LA. Antagonism of AT2 receptors augments angiotensin II-induced abdominal aortic aneurysms and atherosclerosis. Br J Pharmacol 2001;134:865–870. [PubMed: 11606327]
21. Wang, YX.; Cassi, LA.; Daugherty, A. Angiotensin II-induced abdominal aortic aneurysms. In: Xu, EQ., editor. A Handbook of Mouse Models for Cardiovascular Diseases. London: Wiley; 2006. p. 125-146.
22. Flanders KC, Thompson NL, Cissel DS, Van Obberghen-Schilling E, Baker CC, Kass ME, Ellingsworth LR, Roberts AB, Sporn MB. Transforming growth factor-beta 1: histochemical localization with antibodies to different epitopes. J Cell Biol 1989;108:653–660. [PubMed: 2465297]
23. Ng CM, Cheng A, Myers LA, Martinez-Murillo F, Jie C, Bedja D, Gabrielson KL, Hausladen JM, Mecham RP, Judge DP, Dietz HC. TGF-beta-dependent pathogenesis of mitral valve prolapse in a mouse model of Marfan syndrome. J Clin Invest 2004;114:1586–1592. [PubMed: 15546004]
24. Habashi JP, Judge DP, Holm TM, Cohn RD, Loeys BL, Cooper TK, Myers L, Klein EC, Liu G, Calvi C, Podowski M, Neptune ER, Halushka MK, Bedja D, Gabrielson K, Rifkin DB, Carta L, Ramirez F, Huso DL, Dietz HC. Losartan, an AT1 antagonist, prevents aortic aneurysm in a mouse model of Marfan syndrome. Science 2006;312:117–121. [PubMed: 16601194]
25. Bjorkbacka H, Kunjathoor VV, Moore KJ, Koehn S, Ordija CM, Lee MA, Means T, Halmen K, Luster AD, Golenbock DT, Freeman MW. Reduced atherosclerosis in MyD88-null mice links elevated serum cholesterol levels to activation of innate immunity signaling pathways. Nat Med 2004;10:416–421. [PubMed: 15034566]
26. Means T, Hayase F, Luster A. Real time PCR analysis of chemokine receptors. Journal of Immunology. 2002under revision
27. Babamusta F, Rateri DL, Moorleghen JJ, Howatt DA, Li XA, Daugherty A. Angiotensin II infusion induces site-specific intra-laminar hemorrhage in macrophage colony-stimulating factor-deficient mice. Atherosclerosis 2006;186:282–290. [PubMed: 16153649]
28. Saraff K, Babamusta F, Cassis LA, Daugherty A. Aortic dissection precedes formation of aneurysms and atherosclerosis in angiotensin II-infused, apolipoprotein E-deficient mice. Arterioscler Thromb Vasc Biol 2003;23:1621–1626. [PubMed: 12855482]
29. Okamoto Y, Kihara S, Ouchi N, Nishida M, Arita Y, Kumada M, Ohashi K, Sakai N, Shimomura I, Kobayashi H, Terasaka N, Inaba T, Funahashi T, Matsuzawa Y. Adiponectin reduces atherosclerosis in apolipoprotein E-deficient mice. Circulation 2002;106:2767–2770. [PubMed: 12451000]
30. Daugherty A, Cassis L. Chronic angiotensin II infusion promotes atherogenesis in low density lipoprotein receptor −/− mice. Ann N Y Acad Sci 1999;892:108–118. [PubMed: 10842656]
31. Medoff BD, Sauty A, Tager AM, Maclean JA, Smith RN, Mathew A, Dufour JH, Luster AD. IFN-gamma-inducible protein 10 (CXCL10) contributes to airway hyperreactivity and airway inflammation in a mouse model of asthma. J Immunol 2002;168:5278–5286. [PubMed: 11994485]
32. Whitman SC, Ravisankar P, Daugherty A. IFN-gamma deficiency exerts gender-specific effects on atherogenesis in apolipoprotein E−/− mice. J Interferon Cytokine Res 2002;22:661–670. [PubMed: 12162876]
33. Heller EA, Liu E, Tager AM, Yuan Q, Lin AY, Ahluwalia N, Jones K, Koehn SL, Lok VM, Aikawa E, Moore KJ, Luster AD, Gerszten RE. Chemokine CXCL10 promotes atherogenesis by modulating the local balance of effector and regulatory T cells. Circulation 2006;113:2301–2312. [PubMed: 16682613]
34. Daugherty A, Cassis LA. Mouse models of abdominal aortic aneurysms. Arterioscler Thromb Vasc Biol 2004;24:429–434. [PubMed: 14739119]
35. Dufour JH, Dziejman M, Liu MT, Leung JH, Lane TE, Luster AD. IFN-gamma-inducible protein 10 (IP-10; CXCL10)-deficient mice reveal a role for IP-10 in effector T cell generation and trafficking. J Immunol 2002;168:3195–3204. [PubMed: 11907072]
36. Ehrhart EJ, Segarini P, Tsang ML, Carroll AG, Barcellos-Hoff MH. Latent transforming growth factor beta1 activation in situ: quantitative and functional evidence after low-dose gamma-irradiation. Faseb J 1997;11:991–1002. [PubMed: 9337152]

37. Prescott MF, Sawyer WK, Von Linden-Reed J, Jeune M, Chou M, Caplan SL, Jeng AY. Effect of matrix metalloproteinase inhibition on progression of atherosclerosis and aneurysm in LDL receptor-deficient mice overexpressing MMP-3, MMP-12, and MMP-13 and on restenosis in rats after balloon injury. Ann N Y Acad Sci 1999;878:179–190. [PubMed: 10415729]
38. Zhao L, Moos MP, Grabner R, Pedrono F, Fan J, Kaiser B, John N, Schmidt S, Spanbroek R, Lotzer K, Huang L, Cui J, Rader DJ, Evans JF, Habenicht AJ, Funk CD. The 5-lipoxygenase pathway promotes pathogenesis of hyperlipidemia-dependent aortic aneurysm. Nat Med 2004;10:966–973. [PubMed: 15322539]
39. Lemaitre V, Soloway PD, D'Armiento J. Increased medial degradation with pseudo-aneurysm formation in apolipoprotein E-knockout mice deficient in tissue inhibitor of metalloproteinases-1. Circulation 2003;107:333–338. [PubMed: 12538437]
40. Silence J, Collen D, Lijnen HR. Reduced atherosclerotic plaque but enhanced aneurysm formation in mice with inactivation of the tissue inhibitor of metalloproteinase-1 (TIMP-1) gene. Circ Res 2002;90:897–903. [PubMed: 11988491]
41. Wynn TA. Common and unique mechanisms regulate fibrosis in various fibroproliferative diseases. J Clin Invest 2007;117:524–529. [PubMed: 17332879]
42. Saxena V, Lienesch DW, Zhou M, Bommireddy R, Azhar M, Doetschman T, Singh RR. Dual roles of immunoregulatory cytokine TGF-beta in the pathogenesis of autoimmunity-mediated organ damage. J Immunol 2008;180:1903–1912. [PubMed: 18209088]
43. Dai J, Losy F, Guinault AM, Pages C, Anegon I, Desgranges P, Becquemin JP, Allaire E. Overexpression of transforming growth factor-beta1 stabilizes already-formed aortic aneurysms: a first approach to induction of functional healing by endovascular gene therapy. Circulation 2005;112:1008–1015. [PubMed: 16103255]
44. MacTaggart JN, Xiong W, Knispel R, Baxter BT. Deletion of CCR2 but not CCR5 or CXCR3 inhibits aortic aneurysm formation. Surgery 2007;142:284–288. [PubMed: 17689697]
45. Sun J, Sukhova GK, Yang M, Wolters PJ, MacFarlane LA, Libby P, Sun C, Zhang Y, Liu J, Ennis TL, Knispel R, Xiong W, Thompson RW, Baxter BT, Shi GP. Mast cells modulate the pathogenesis of elastase-induced abdominal aortic aneurysms in mice. J Clin Invest 2007;117:3359–3368. [PubMed: 17932568]
46. Tsunemi K, Takai S, Nishimoto M, Yuda A, Hasegawa S, Sawada Y, Fukumoto H, Sasaki S, Miyazaki M. Possible roles of angiotensin II-forming enzymes, angiotensin converting enzyme and chymase-like enzyme, in the human aneurysmal aorta. Hypertens Res 2002;25:817–822. [PubMed: 12484503]
47. Hackam DG, Thiruchelvam D, Redelmeier DA. Angiotensin-converting enzyme inhibitors and aortic rupture: a population-based case-control study. Lancet 2006;368:659–665. [PubMed: 16920471]
48. Jones GT, Thompson AR, van Bockxmeer FM, Hafez H, Cooper JA, Golledge J, Humphries SE, Norman PE, van Rij AM. Angtiotensin II type 1 receptor 1166C polymorphism is associated with abdominal aortic aneurysm in three independent cohorts. Aterioscler Thromb Vasc Biol. 2008
49. Fatini C, Pratesi G, Sofi F, Gensini F, Sticchi E, Lari B, Pulli R, Dorigo W, Azas L, Pratesi C, Gensini GF, Abbate R. ACE DD genotype: a predisposing factor for abdominal aortic aneurysm. Eur J Vasc Endovasc Surg 2005;29:227–232. [PubMed: 15694792]

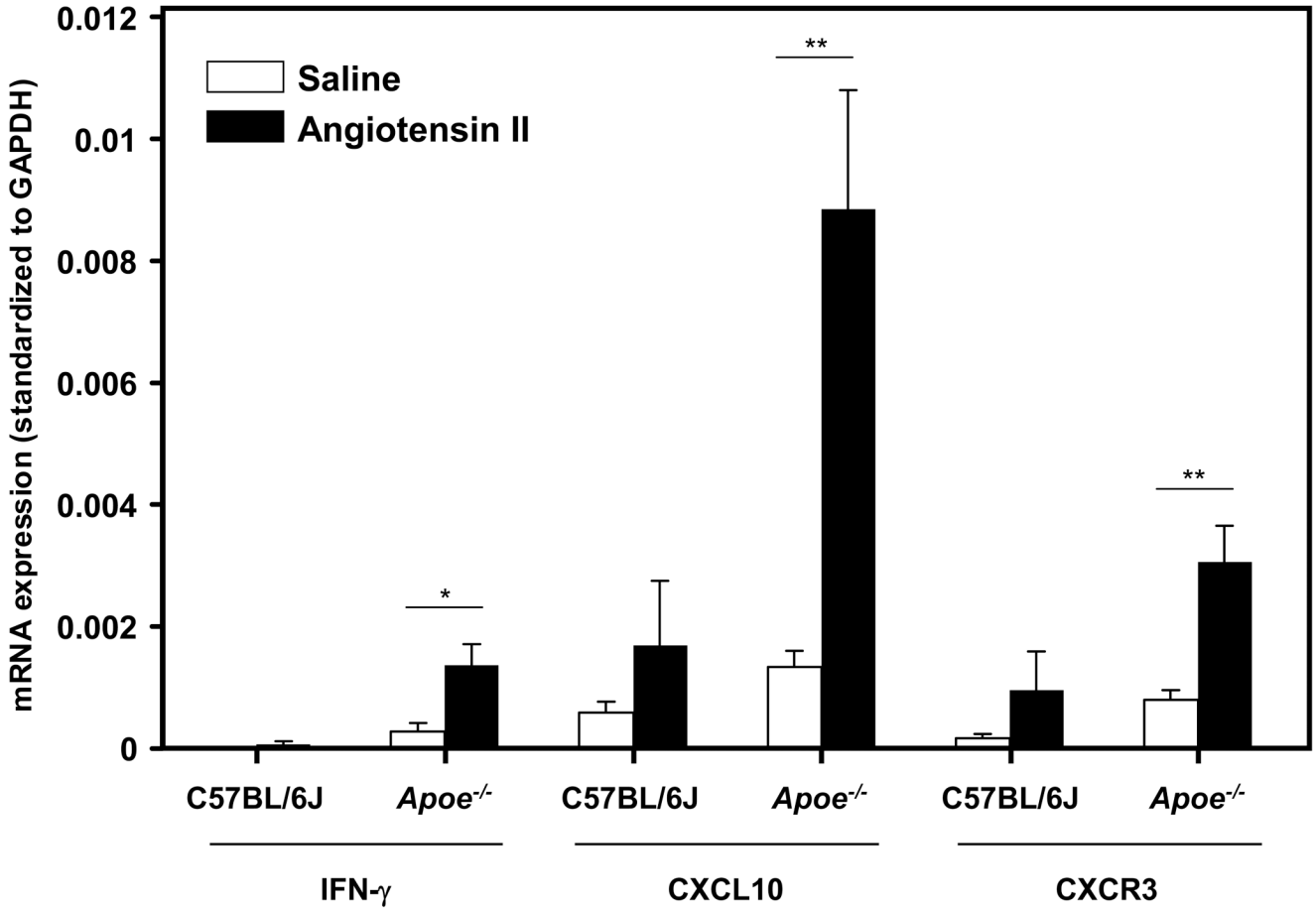

Figure 1. Ang II-treated Apoe$^{-/-}$ mice have increased levels of Th1-associated cytokines

qPCR of aortic segments from C57BL/6J and *Apoe*$^{-/-}$ mice infused with AngII (1000 ng·kg^{-1}·min^{-1}) (closed bars) versus saline (open bars). Data are standardized to GAPDH values. Th1-related cytokines: IFN-γ, CXCL10, and its receptor, CXCR3 ($n \geq 6$ per condition, *P<0.05, **P<0.01).

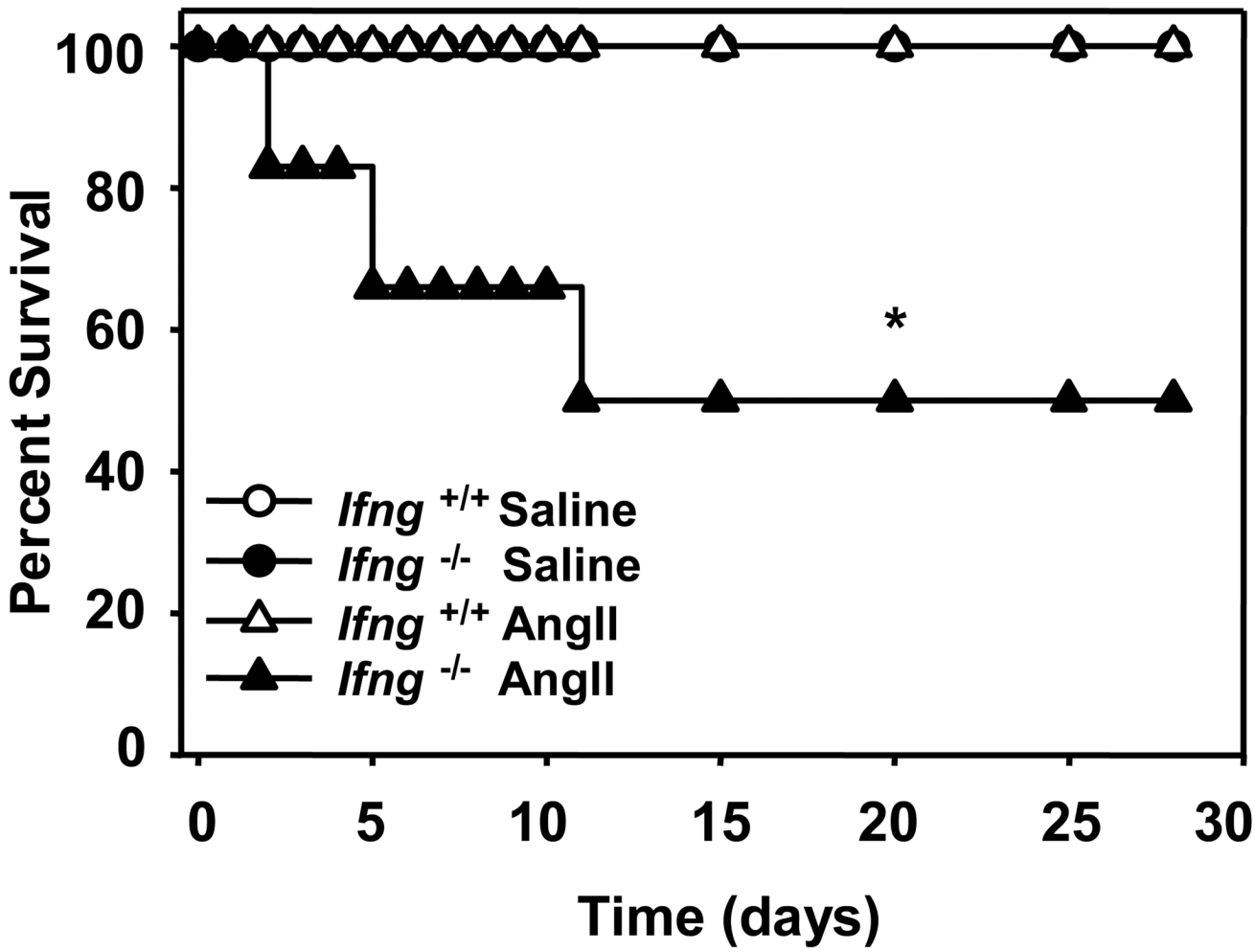

Figure 2. IFN-γ deficiency increased mortality due to aneurysmal rupture in AngII-infused $Apoe^{-/-}$ mice

AngII (1000 $ng \cdot kg^{-1} \cdot min^{-1}$) or saline was infused for 28 days via Alzet minipumps implanted subcutaneously into $Apoe^{-/-}/Ifng^{+/+}$ or $Apoe^{-/-}/Ifng^{-/-}$ mice. Data represent the percent survival in $Apoe^{-/-}/Ifng^{+/+}$ (open symbols, n = 11) or $Apoe^{-/-}/Ifng^{-/-}$ (closed symbols, n = 11) mice following infusion with saline (circles, n = 5 mice/group) or AngII (triangles, n = 6 mice/group). *P<0.05 for AngII-infused $Apoe^{-/-}/Ifng^{+/+}$ compared to $Apoe^{-/-}/Ifng^{-/-}$. Note is made that there were no deaths in either of the saline treated groups nor in the AngII-infused $Ifng^{+/+}$ mice, and thus the symbols representing these groups are superimposed.

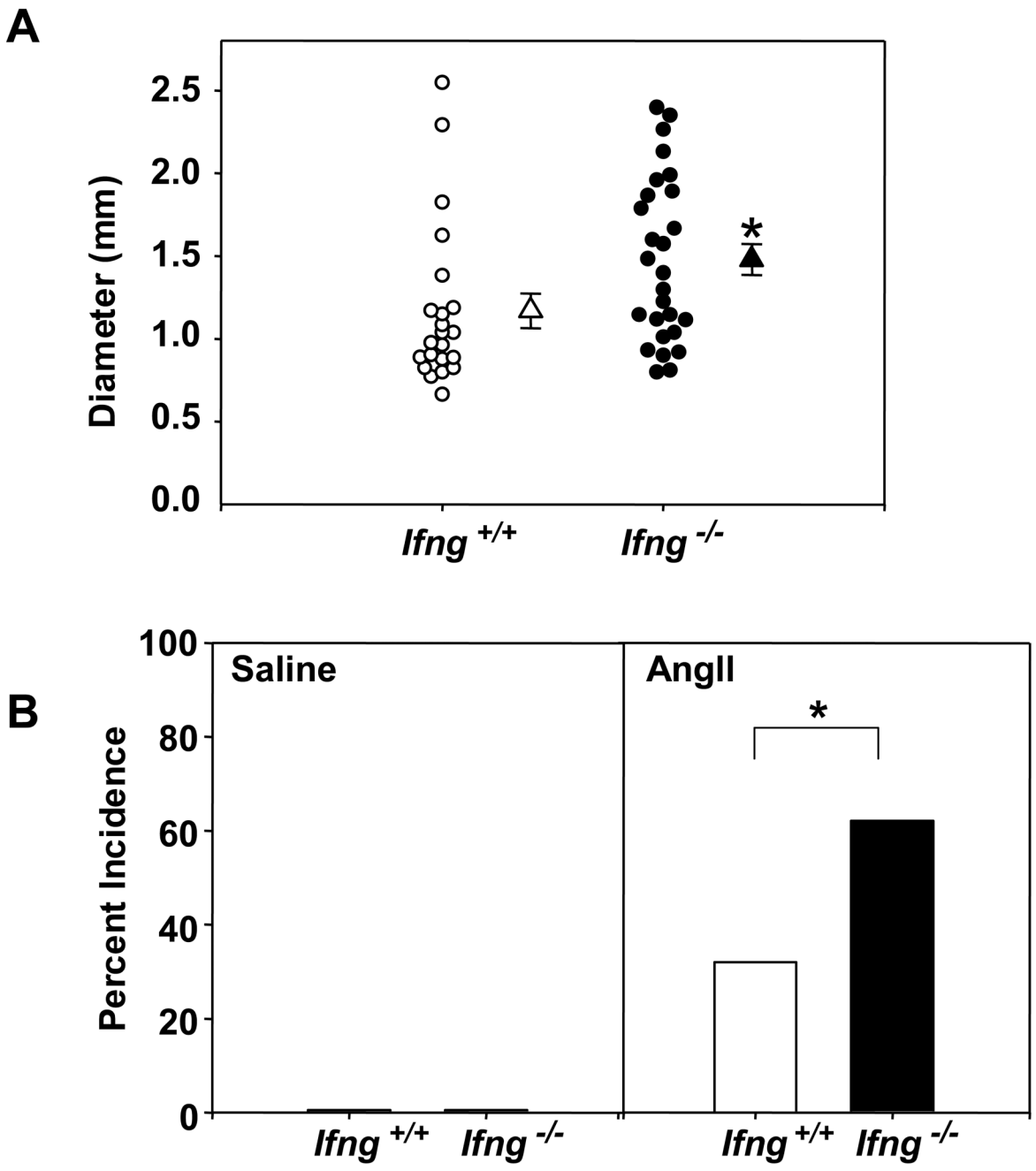

Figure 3. IFN-γ deficiency augmented AngII-induced AAA formation

(**A**). Circles represent suprarenal aortic diameter in individual mice and triangles are the mean ± SEM of *Apoe*$^{-/-}$/*Ifng*$^{+/+}$ (open symbols) and *Apoe*$^{-/-}$/*Ifng*$^{-/-}$ (closed symbols) mice infused with AngII (500 ng·kg^{-1}·min $^{-1}$; *Apoe*$^{-/-}$/*Ifng*$^{+/+}$: n = 25; *Apoe*$^{-/-}$/*Ifng*$^{-/-}$: n = 29 mice). Data were analyzed by Mann-Whitney Rank Sum test. *P<0.05. (**B**) Data represent the percent incidence of AAAs in *Apoe*$^{-/-}$/*Ifng*$^{+/+}$ (open bars; saline: n = 8; AngII: n = 25) and *Apoe*$^{-/-}$/*Ifng*$^{-/-}$ (closed bars; saline: n = 8; AngII: n = 29). Data were analyzed by Fisher's Exact Test. *P<0.05 for AngII-infused *Apoe*$^{-/-}$/*Ifng*$^{+/+}$ compared to *Apoe*$^{-/-}$/*Ifng*$^{-/-}$.

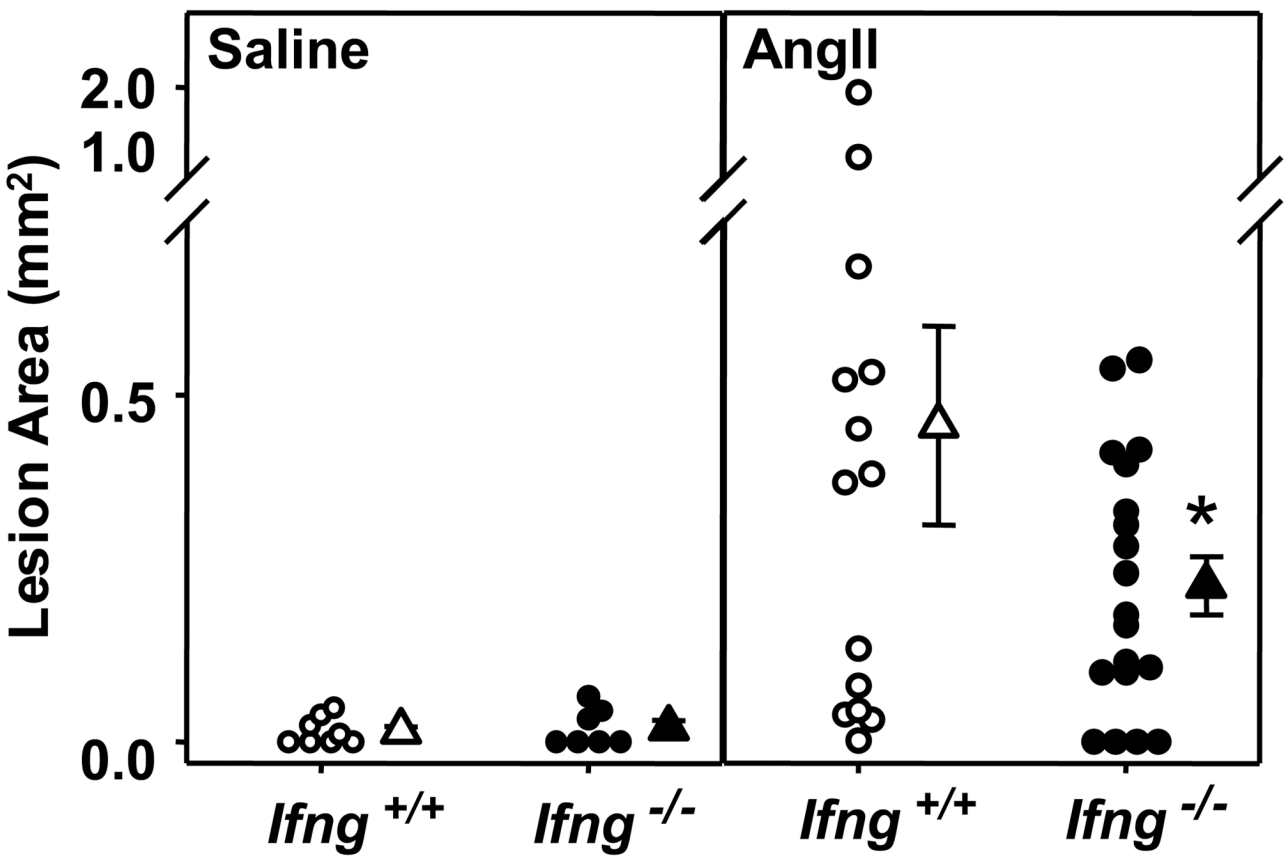

Figure 4. IFN-γ deficiency attenuated AngII-induced atherosclerosis

Atherosclerotic lesion size was determined on the intimal surface of the aorta extending from the aortic arch to the last intercostal artery branch in the thorax in *Apoe*$^{-/-}$/*Ifng*$^{+/+}$ and *Apoe*$^{-/-}$/*Ifng*$^{-/-}$ mice infused with AngII (500 ng·kg^{-1}·min^{-1}) or saline for 28 days. Lesion size was determined irrespective of the presence or absence of AAA; only mice that expired from AAA rupture were omitted from this analysis. Circles represent measurements from individual mice and triangles are the mean lesion area ± SEM of *Apoe*$^{-/-}$/*Ifng*$^{+/+}$ (open symbols; saline: n = 8, AngII: n = 14) and *Apoe*$^{-/-}$/*Ifng*$^{-/-}$ (closed symbols; saline: n = 7, AngII: n = 19) mice. *P<0.05 for AngII-infused *Apoe*$^{-/-}$/*Ifng*$^{+/+}$ compared to *Apoe*$^{-/-}$/*Ifng*$^{-/-}$. Data were analyzed by 2-way ANOVA.

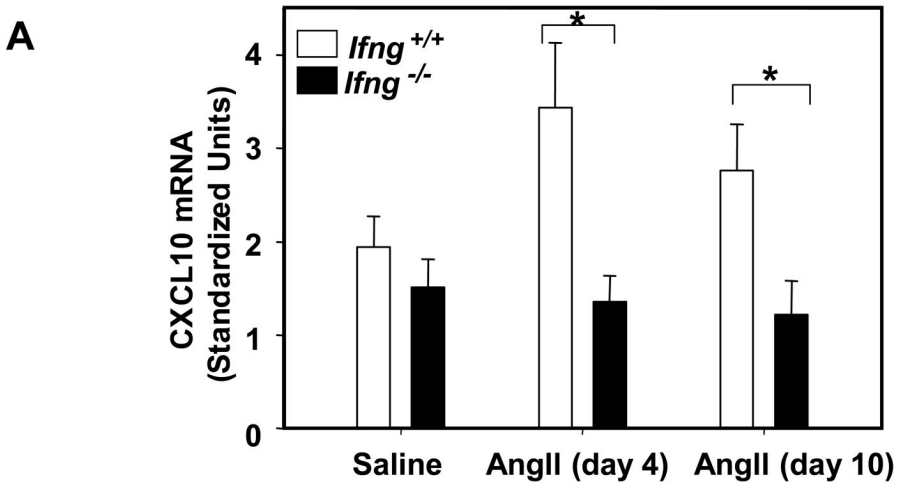

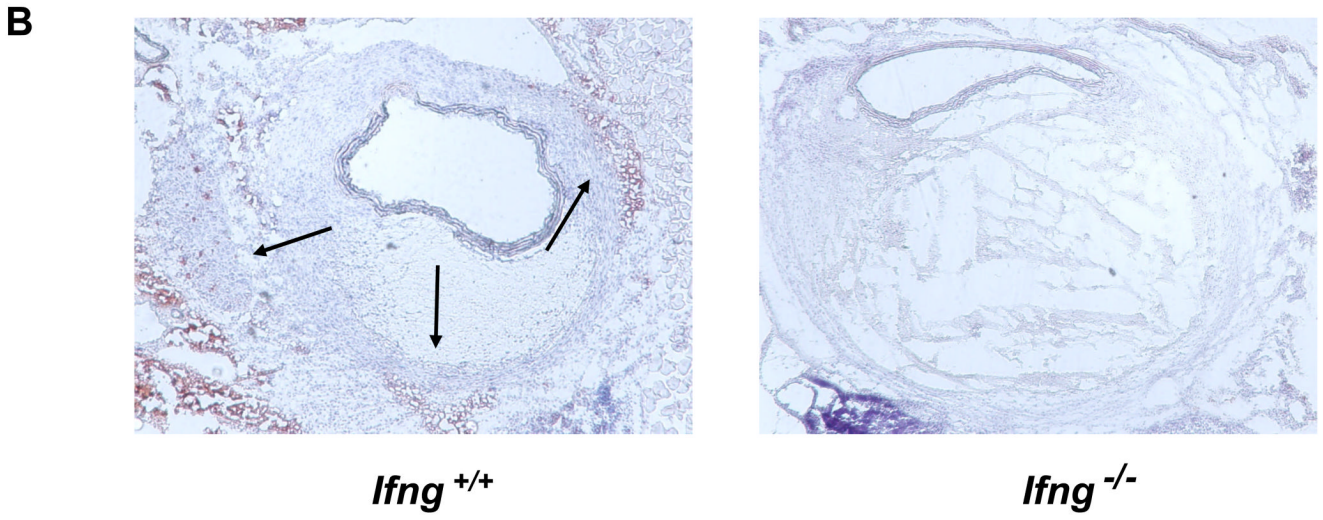

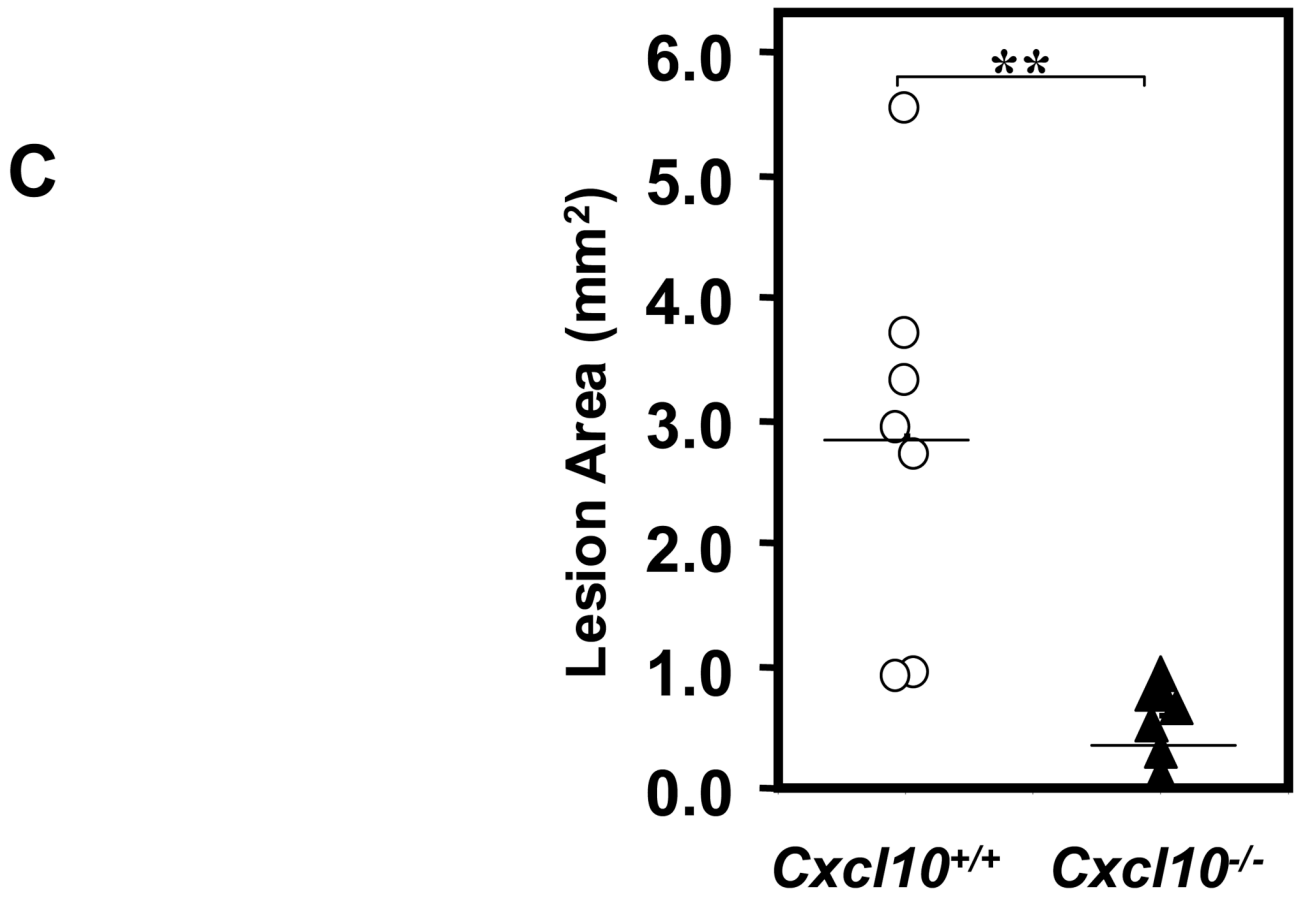

Figure 5. Decreased CXCL10 expression in IFN-γ-deficient mice; decreased atherosclerotic plaque in CXCL10-deficient mice

(**A**) qPCR of CXCL10 expression in the spleen from *Apoe*$^{-/-}$/*Ifng*$^{+/+}$ (open bars) and *Apoe*$^{-/-}$/*Ifng*$^{-/-}$ (closed bars) mice infused with AngII (500 ng·kg^{-1}·min^{-1}) for 4 or 10 days versus saline (n = 5 mice/group, *P<0.05). (**B**) Immunohistochemical analysis of CXCL10 in representative lesions from *Apoe*$^{-/-}$/*Ifng*$^{+/+}$ and *Apoe*$^{-/-}$/*Ifng*$^{-/-}$ mice. (**C**) Atherosclerotic lesion size was determined on the intimal surface of the aorta extending from the aortic arch to the last intercostal artery branch in the thorax in *Apoe*$^{-/-}$/*Cxcl10*$^{+/+}$ (circles, n = 7) and *Apoe*$^{-/-}$/*Cxcl10*$^{-/-}$ (triangles, n = 7) mice infused with AngII (1000 ng·kg^{-1}·min^{-1}) for 28 days. Lesion size was determined irrespective of the presence or absence of AAA; only mice that expired from AAA rupture were omitted from this analysis. **P<0.005 for AngII-infused *Apoe*$^{-/-}$/*Cxcl10*$^{+/+}$ compared to *Apoe*$^{-/-}$/*Cxcl10*$^{-/-}$. Data were analyzed by 2-way ANOVA.

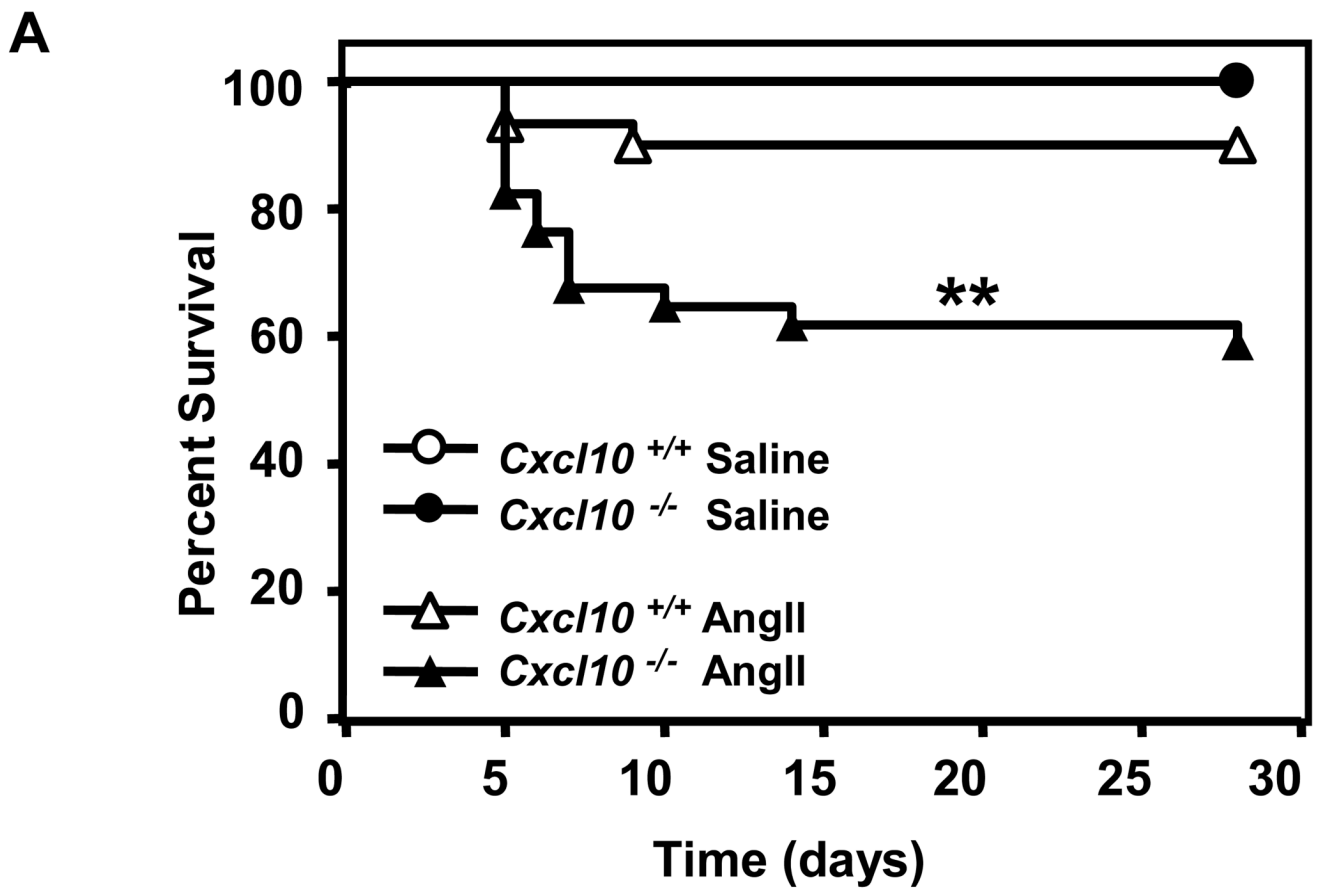

B

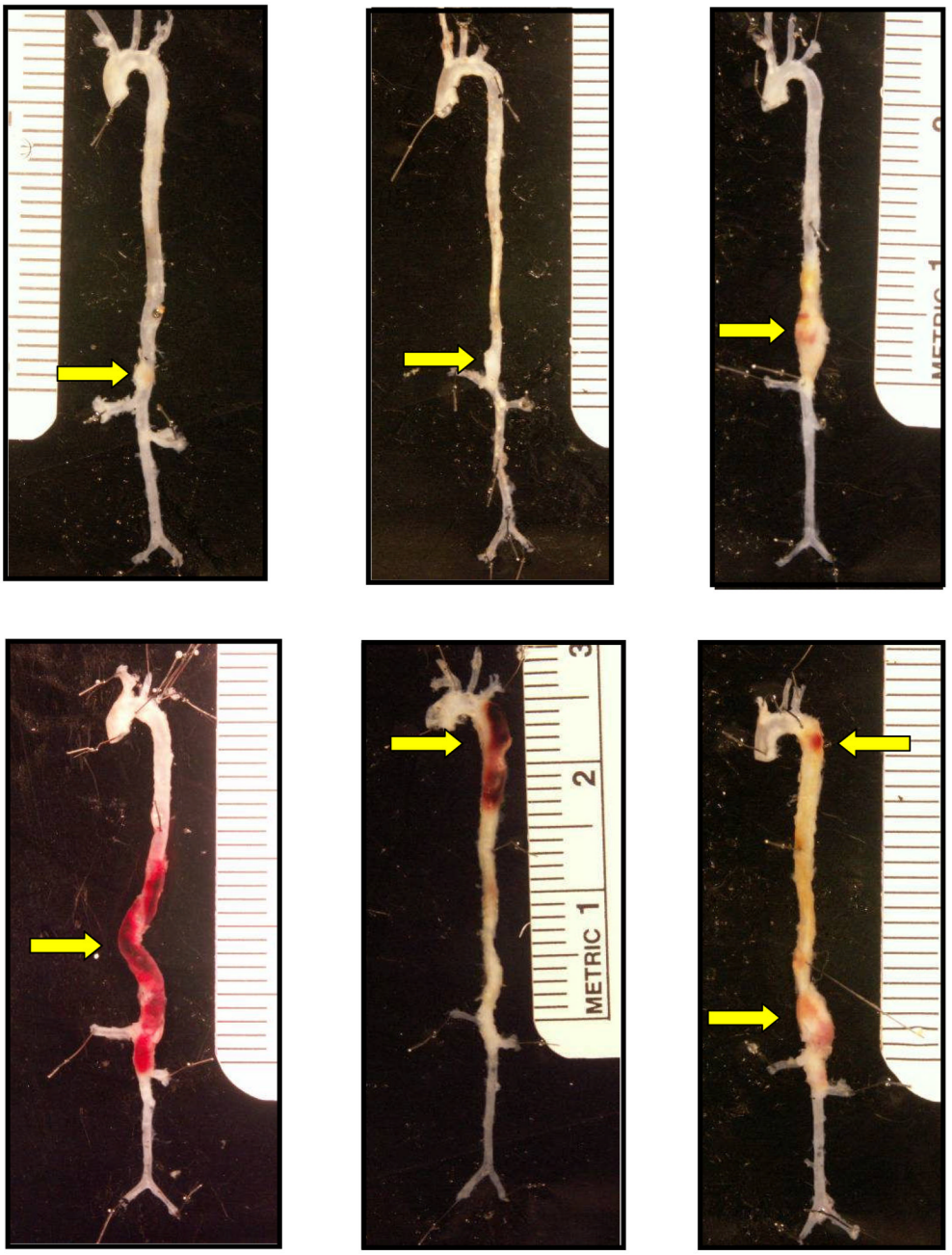

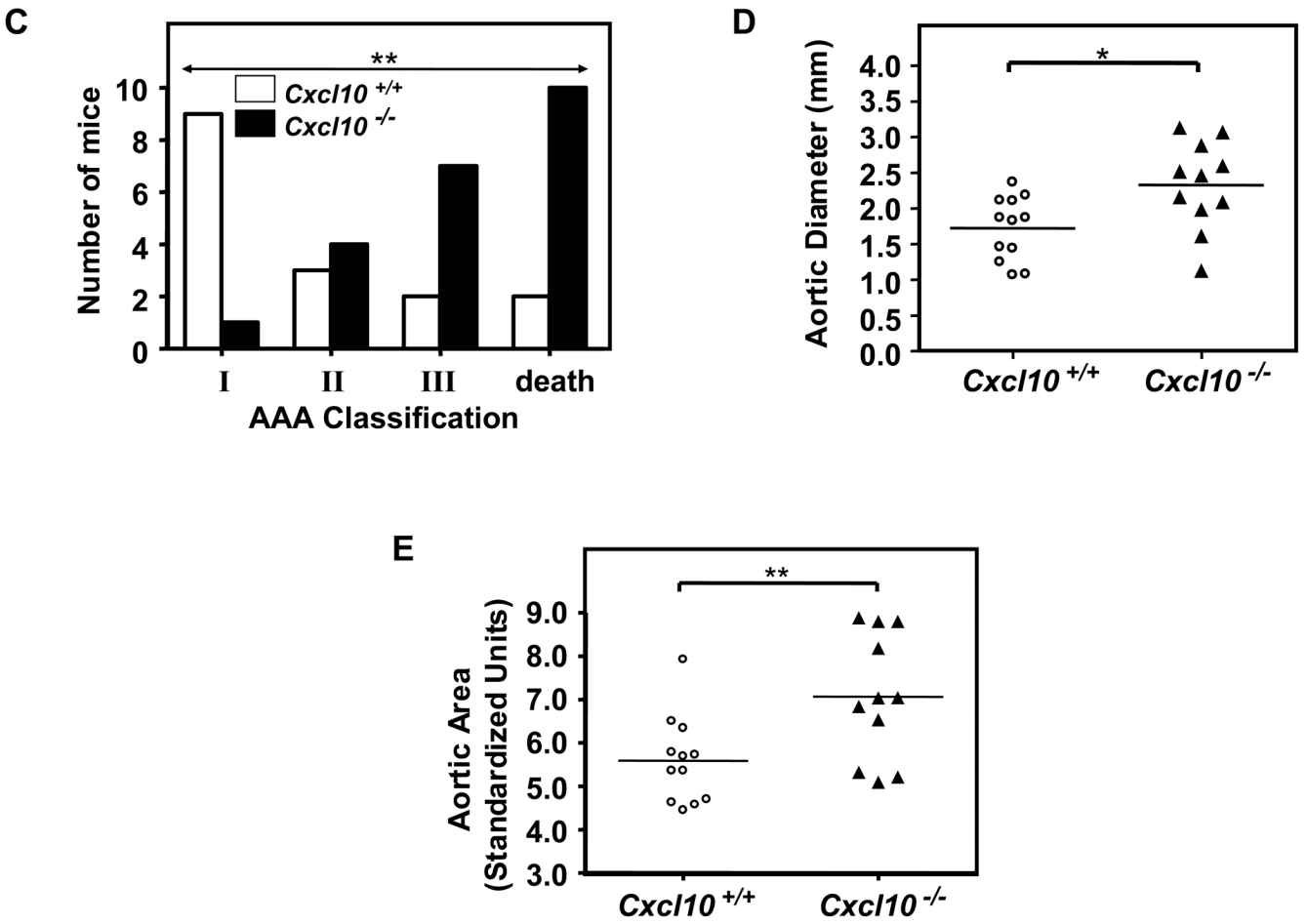

Figure 6. Increased mortality and severity of AAAs in CXCL10-deficient mice

(**A**) AngII (1000 ng·kg^{-1}·min^{-1}) or saline was infused for 28 days into *Apoe*$^{-/-}$/*Cxcl10*$^{+/+}$ or *Apoe*$^{-/-}$/*Cxcl10*$^{-/-}$ mice. Data represent the percent survival in *Apoe*$^{-/-}$/*Cxcl10*$^{+/+}$ (open symbols, n = 30) or *Apoe*$^{-/-}$/*Cxcl10*$^{-/-}$ (closed symbols, n = 36) mice following infusion with saline (circles, n = 6 mice per genotype) or AngII (triangles, *Apoe*$^{-/-}$/*Cxcl10*$^{+/+}$, n = 18; *Apoe*$^{-/-}$/*Cxcl10*$^{-/-}$, n = 24) **P<0.01. (**B**) Representative aortas from *Apoe*$^{-/-}$/*Cxcl10*$^{+/+}$mice (upper row) and *Apoe*$^{-/-}$/*Cxcl10*$^{-/-}$ mice (bottom row), with arrows pointing to abdominal and thoracic aneurysms, with an example of a spiral dissection (lower left). (**C**) Histobars represent the severity of AAAs in *Apoe*$^{-/-}$/*Cxcl10*$^{+/+}$ (open bars) and *Apoe*$^{-/-}$/*Cxcl10*$^{-/-}$ (closed bars) mice based on morphological classification (see Methods) (*Apoe*$^{-/-}$/*Cxcl10*$^{+/+}$, n = 16; *Apoe*$^{-/-}$/*Cxcl10*$^{-/-}$, n = 22 mice). **P<0.01 by Chi Square analysis. (**D**) Circles (*Apoe*$^{-/-}$/*Cxcl10*$^{+/+}$, n = 12) and triangles (*Apoe*$^{-/-}$/*Cxcl10*$^{-/-}$, n = 11) represent the suprarenal aortic diameters in individual mice infused with AngII (1000 ng·kg^{-1}·min^{-1}) for 28 days. Data were analyzed by Mann-Whitney Rank Sum test. *P<0.05. (**E**) Circles (*Apoe*$^{-/-}$/*Cxcl10*$^{+/+}$, n = 12) and triangles (*Apoe*$^{-/-}$/*Cxcl10*$^{-/-}$, n = 11) represent the ratios of the suprarenal/thoracic to infrarenal aortic areas in individual mice infused with AngII (1000 ng·kg^{-1}·min^{-1}). Data were analyzed by Mann-Whitney Rank Sum test. **P<0.01.

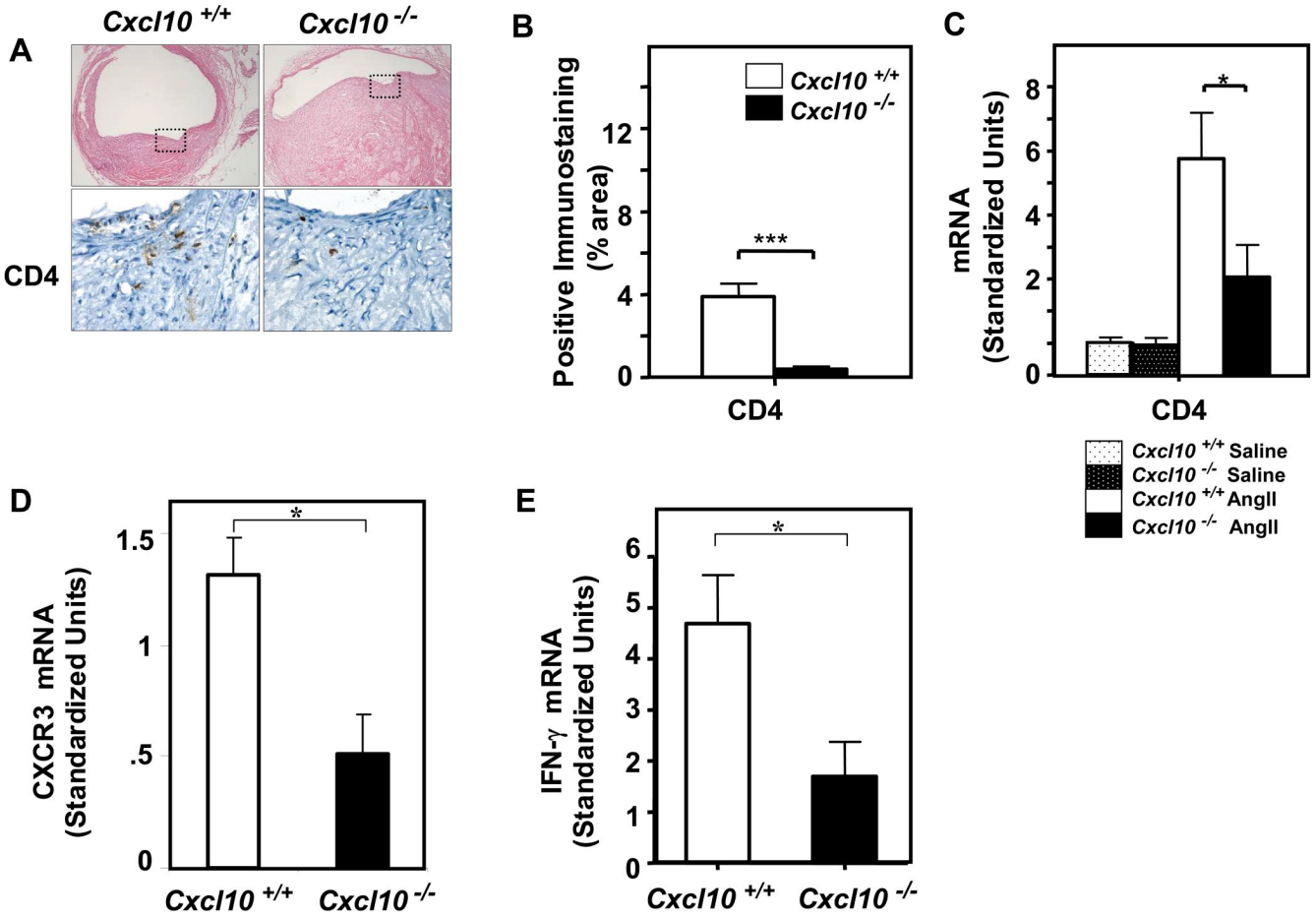

Figure 7. CXCL10 deficiency attenuates AngII-induced T cell infiltration into the vascular wall

Immunostaining analysis of aneurysms from *Apoe*$^{-/-}$/*Cxcl10*$^{+/+}$ or *Apoe*$^{-/-}$/*Cxcl10*$^{-/-}$ mice infused with AngII (1000 ng·kg^{-1}·min^{-1}) or saline for 28 days. (**A**) Representative cross-sections (40X) of the suprarenal aorta from *Apoe*$^{-/-}$/*Cxcl10*$^{+/+}$ (left top panel) or *Apoe*$^{-/-}$/*Cxcl10*$^{-/-}$ (right top panel) mice. Boxed area is expanded to show representative high-power fields (HPFs) with immunostaining for T lymphocytes in serial sections (CD4, lower panels). (**B**) Quantification of immunostaining (5 or more fields/slide) from *Apoe*$^{-/-}$/*Cxcl10*$^{+/+}$ (open bar) or *Apoe*$^{-/-}$/*Cxcl10*$^{-/-}$ (closed bar) mice (n ≥ 3 mice/group). Data are normalized to lesion area (***P<0.0001 and **P<0.01). (**C**) qPCR analysis of CD4 mRNA expression in suprarenal aortas from *Apoe*$^{-/-}$/*Cxcl10*$^{+/+}$ or *Apoe*$^{-/-}$/*Cxcl10*$^{-/-}$ mice (n ≥ 6 mice/group; *P<0.05). (**D**) qPCR analysis of CXCR3 mRNA expression in the suprarenal aorta from *Apoe*$^{-/-}$/*Cxcl10*$^{+/+}$ and *Apoe*$^{-/-}$/*Cxcl10*$^{-/-}$ mice (n ≥ 10 mice/group; *P<0.05). (**E**) qPCR analysis of IFN-γ mRNA expression in the suprarenal aorta from *Apoe*$^{-/-}$/*Cxcl10*$^{+/+}$ and *Apoe*$^{-/-}$/*Cxcl10*$^{-/-}$ mice (n ≥ 10 mice/group; *P<0.05).

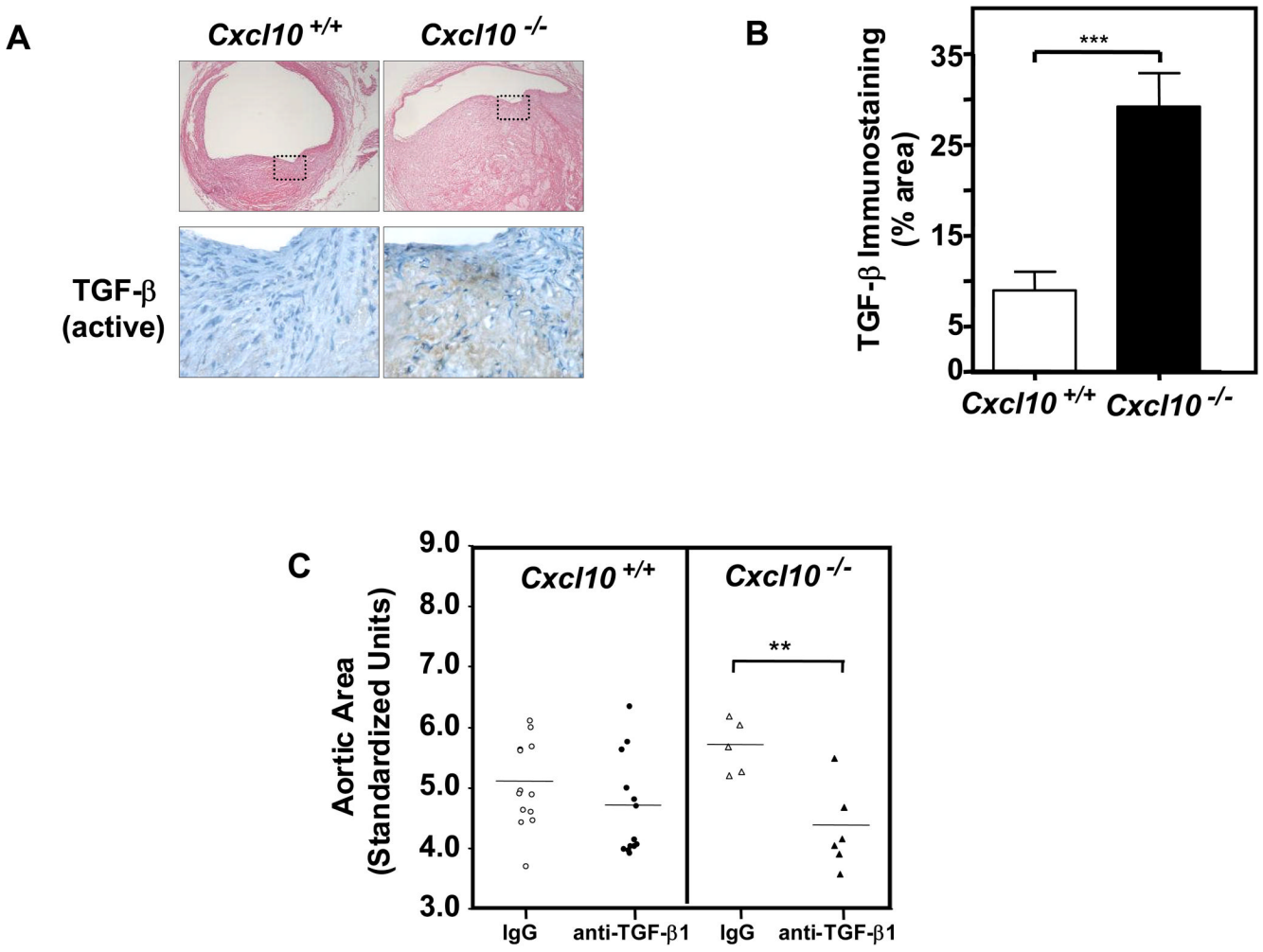

Figure 8. Enhanced TGF-β activation contributes to worse AAA in CXCL10-deficient mice

(**A**) Representative cross-sections of the suprarenal aorta from AngII-infused *Apoe*$^{-/-}$/*Cxcl10*$^{+/+}$ (left panel) and *Apoe*$^{-/-}$/*Cxcl10*$^{-/-}$ (right panel) mice were immunostained with an activation-specific TGF-β antibody (bottom panels). (**B**) Quantification of active TGF-β immunostaining from *Apoe*$^{-/-}$/*Cxcl10*$^{+/+}$ (open bar) or *Apoe*$^{-/-}$/*Cxcl10*$^{-/-}$ (closed bar) mice ($n \geq 3$ mice/group; ***P<0.0001). (**C**) *Apoe*$^{-/-}$/*Cxcl10*$^{+/+}$ and *Apoe*$^{-/-}$/*Cxcl10*$^{-/-}$ mice were infused with AngII (1000 ng·kg^{-1}·min^{-1}) for 14 days. Anti-TGF-β neutralizing Ab (1 mg/kg; closed symbols) or IgG isotype control (1 mg/kg; open symbols) was administered by IP injection on the day before pump placement and the day following. Circles (*Apoe*$^{-/-}$/*Cxcl10*$^{+/+}$, n=24) and triangles (*Apoe*$^{-/-}$/*Cxcl10*$^{-/-}$, n=11) represent the ratios of the suprarenal/thoracic to infrarenal aortic areas in individual mice. Data were analyzed by Mann-Whitney Rank Sum. **P<0.01.

Table 1

Analysis of Baseline Characteristics Between Apoe$^{-/-}$ and Apoe$^{-/-}$/Ifng$^{-/-}$ Mice.

Infusion	IFN-γ Genotype	n	Cholesterol (mg/dl)	Body Weight (g)
Saline	+/+	8	328 ± 15	27.1 ± 0.7
	−/−	8	318 ± 21	30.8 ± 1.1*
AngII (500 ng·kg^{-1}·min^{-1})	+/+	17	286 ± 17	27.9 ± 0.8
	−/−	19	327 ± 12	30.5 ± 0.4*

Data represent means ± SEM.

*$P < 0.001$ for *Apoe*$^{-/-}$/*Ifng*$^{+/+}$ compared to *Apoe*$^{-/-}$/*Ifng*$^{-/-}$ mice within saline and AngII-infused groups.

Table 2

Analysis of Baseline Characteristics Between Apoe$^{-/-}$ and Apoe$^{-/-}$/Cxcl10$^{-/-}$ Mice.

Infusion	CXCL10 Genotype	n	Cholesterol (mg/dl)	Body Weight (g)
Saline	+/+	5	437 ± 48	24.3 ± 0.4
	−/−	4	510 ± 63	25.2 ± 2.5
AngII (1000 ng·kg^{-1}·min^{-1})	+/+	30	535 ± 33	26.6 ± 0.8
	−/−	23	455 ± 30	29.2 ± 0.9*

Data represent means ± SEM.

* P < 0.05 for *Apoe*$^{-/-}$/*Cxcl10*$^{+/+}$ compared to *Apoe*$^{-/-}$/*Cxcl10*$^{-/-}$ mice within saline and AngII-infused groups.